# Influence of Model Parameter Uncertainty on Seismic Transverse Response and Vulnerability of Steel–Concrete Composite Bridges with Dual Load Path

E. Tubaldi[1]; M. Barbato, M.ASCE[2]; and A. Dall'Asta[3]

**Abstract:** This paper uses a fully probabilistic approach to investigate the seismic response of multispan continuous bridges with dissipative piers and a steel–concrete composite (SCC) deck, the motion of which is transversally restrained at the abutments. This bridge typology is characterized by complex dual load path behavior in the transverse direction, with multiple failure modes involving both the deck and the piers. Proper assessment of the seismic vulnerability of these structural systems must rigorously take into account all pertinent sources of uncertainty, including uncertainties in both the seismic input (record-to-record variability) and the properties defining the structural model (model parameters). Model parameter uncertainty affects not only the structural capacity, but also the seismic response of a structural system. However, most of the procedures for seismic vulnerability assessment focus on the variability of the response resulting solely from seismic input uncertainty. These procedures either neglect model parameter uncertainty effects or incorporate these effects only in a simplified way. A computationally expensive but rigorous procedure is introduced in this work to include the effects of model parameter uncertainty on the seismic response and vulnerability assessment of SCC bridges with dual load path. Monte Carlo simulation with Latin hypercube sampling, in conjunction with probabilistic moment–curvature analysis, is used to build probabilistic finite-element models of the bridges under study. Extended incremental dynamic analysis is used to propagate all pertinent sources of uncertainty to the seismic demand. The proposed procedure is then applied to the assessment of three benchmark bridges exhibiting different seismic behavior and dominant failure modes. Comparison of the response variability induced by seismic input uncertainty and the response variability induced by model parameter uncertainty highlights the importance of accounting for the latter when evaluating the safety of the typology of bridges considered in this study.
**DOI: 10.1061/(ASCE)ST.1943-541X.0000456.** 

**CE Database subject headings:** Steel; Concrete; Composite bridges; Finite element method; Seismic effects; Dynamic analysis; Earthquake engineering; Load factors; Uncertainty principles.

**Author keywords:** Steel-concrete composite structures; Bridges; Nonlinear finite element method; Seismic behavior; Incremental dynamic analysis; Performance-based earthquake engineering.

## Introduction

Steel–concrete composite (SCC) bridges are a very common, economical, and efficient type of highway bridge, especially in the range of short and medium span lengths (Collings 2005). These bridges are usually characterized by a continuous SCC deck resting on reinforced concrete piers (Itani et al. 2003), the latter providing the main seismic energy dissipation source. The seismic performance of this bridge typology during recent earthquakes has been extensively discussed in many studies (Astaneh-Asl et al. 1994; Kawashima 2010). Numerical investigation of their seismic response has also been carried out, as in Padgett and DesRoches (2008). These studies have highlighted the likelihood of damage to the various components that lie in the seismic load paths, including the piers, the deck, and the bearings.

To reduce deck bending and avoid expensive bidirectional joints, a rigid connection can be established between the deck and the abutments by means of fixed bearings, steel-plate stoppers, or special links restraining the transverse displacements [European Committee for Standardization (ECS) 2005]. In this situation, "dual load path" transverse behavior is observed (Calvi 2004; Tubaldi et al. 2010), with two different mechanisms resisting the earthquake-induced inertia forces. These two mechanisms are (1) the inelastic load path constituted by the piers, designed to yield and dissipate the input energy; and (2) the elastic load path formed by the deck and the abutments, designed to remain elastic according to capacity design principles [ECS 2005; Federation Internationale du Beton (FIB) 2007]. A recent parametric study (Tubaldi et al. 2010) analyzed changes in the seismic response of multispan continuous SCC bridges with dual load path caused by a variation in the relative deck-to-pier stiffness ratio. The influence of relative stiffness on global response was investigated by varying the ratio $H/D$ between the height $H$ and the cross-section diameter $D$ of the piers. Only uncertainty in seismic input was considered by subjecting the bridges to different sets of ground motions characterized by variable intensity and frequency content. The following

[1]Post Doctoral Researcher, Dipartimento di Architettura Costruzione e Strutture, Università Politecnica delle Marche, Via Brecce Bianche 60131, Ancona, Italy. E-mail: etubaldi@libero.it

[2]Assistant Professor, Dept. of Civil & Environmental Engineering, Louisiana State Univ. and A&M College, 3531 Patrick F. Taylor Hall, Nicholson Extension, Baton Rouge, LA 70803, USA (corresponding author). E-mail: mbarbato@lsu.edu

[3]Professor, Scuola di Architettura e Design, Univ. of Camerino, Viale della Rimembranza 63100, Ascoli Piceno (AP), Italy. E-mail: andrea.dallasta@unicam.it

Note. This manuscript was submitted on April 2, 2010; approved on June 15, 2011; published online on June 17, 2011. Discussion period open until August 1, 2012; separate discussions must be submitted for individual papers. This paper is part of the ***Journal of Structural Engineering***, Vol. 138, No. 3, March 1, 2012. ©ASCE, ISSN 0733-9445/2012/3-363–374/$25.00.

results were obtained: (1) the elastic load path assumes an increasing importance relative to the inelastic one for increasing values of $H/D$; (2) different dispersions characterize the strength and deformation demand at the different resisting components; (3) multiple failure modes, involving different components, must be considered when analyzing these bridges; and (4) failure can be reached as a result of deck yielding or exceedance of the curvature capacity of the piers, depending on the ratio $H/D$.

The difference observed in the failure modes and in the statistics of the monitored engineering demand parameters (EDPs), for the various geometric configurations (i.e., $H/D$ ratios) analyzed in Tubaldi et al. (2010), suggested that uncertainty affecting input ground motion and model parameters can play an important role in structural safety and deserves further investigation. To investigate these effects, a fully probabilistic procedure must be defined and employed to propagate these uncertainties through the response and vulnerability assessment of the various geometric configurations analyzed.

Previous studies by other researchers have recognized the importance of model parameter uncertainty to structural performance and have developed appropriate methodologies for evaluating the effects of model parameter uncertainty on seismic response (Hwang and Jaw 1990; Dymiotis et al. 1999; Padgett and DesRoches 2007; Dolsek 2009; Vamvatsikos and Fragiadakis 2010). However, these methodologies have been specifically developed for structural typologies other than that considered in this study. Most of these studies focused on the performance of building frames, whereas Padgett and DesRoches (2007) investigated the performance of existing bridges retrofitted according to various techniques.

The main goal of the present study is to investigate the seismic response and fragility of SCC bridges with dual load path by considering uncertainty related to both ground motion and model parameters. In addition, this study aims to identify and quantify the role of the different sources of uncertainty in the variability of the seismic response and vulnerability of SCC bridges with dual load path.

The uncertainties considered in the study are divided into two categories on the basis of their different numerical treatment: ground motion uncertainty (or simply randomness, $R$), and model parameter uncertainty (or simply uncertainty, $U$). Randomness $R$ is the uncertainty of aleatoric nature related to seismic input (e.g., as a result of frequency content, duration, and record-to-record variability of ground motion) that can affect a given structure (Katsanos et al. 2010). Uncertainty $U$ is a combination of aleatoric and epistemic uncertainty (Padgett and DesRoches 2007), and includes the intrinsic variability of geometric and material parameters defining the system (e.g., material constitutive properties, cross-section dimensions), modeling assumptions, and lack of knowledge (e.g., plastic hinge length). These sources of variability affect both the demand on and the capacity of the bridge components.

In this paper, a rigorous methodology to evaluate the effects of model parameter uncertainty is proposed and specifically developed for the probabilistic problem considered. This methodology innovatively combines existing techniques, previously developed by other researchers for different types of structures, and represents a novel application of these techniques to bridge engineering. It uses a computationally efficient Latin hypercube sampling to reproduce the variability of model parameter uncertainty. It is noteworthy that the proposed methodology is able to account for multiple limit states, similar to the technique proposed in Padgett and DesRoches (2007). However, in contrast to the work of Padgett and DesRoches (2007), the newly proposed methodology uses a direct simulation approach and, thus, does not require the introduction of any assumption (e.g., lognormality) on the statistical distribution of the seismic demand. Moreover, as opposed to traditional approaches, the proposed procedure is capable of accounting for the dependence of both demand and capacity on uncertainty $U$ and, thus, of simulating their joint probability distribution. This innovative feature is accomplished through the use of probabilistic moment–curvature analysis of the most critical resisting components, which is employed to generate a probabilistic model of the capacity of the structural components and to define the probabilistic finite-element (FE) model. The use of concentrated plasticity models, instead of a fiber-based model, provides a good compromise between accuracy, complexity, and speed of computation, the last being required by the large number of nonlinear FE analyses involved.

The methodology is applied to the seismic response and fragility assessment of a set of multispan continuous SCC bridges with dual load path having different geometric configurations (i.e., $H/D$ ratios of the piers). These bridges are characterized by a different response and fragility of the system and of the components involved in the two load paths. The sensitivity of the response with respect to model parameters is studied to highlight the parameters that most significantly influence the seismic behavior of the bridges. Furthermore, the effects of $U$ and $R$ on the variability of the demand are evaluated jointly and separately with the aim of investigating the suitability of simplified approaches for reducing the computational cost of the analyses.

## Methodology

This paper employs the extended incremental dynamic analysis (EIDA) method (Dolsek 2009; Vamvatsikos and Fragiadakis 2010) for propagating uncertainties from model parameters and seismic ground motion to the EDPs used to monitor the system response. EIDA couples ordinary incremental dynamic analysis (IDA) (Vamvatsikos and Cornell 2002) with a simulation technique used to generate a probabilistic FE model of the structural system under study. Randomness is modeled through the selection of a sufficiently large number, $N_{gm}$, of recorded ground accelerations appropriately chosen from the Internet database of the Pacific Earthquake Engineering Research Center (PEER 2006). Uncertainty is described by modeling a wide range of model parameters as random variables (RVs), assuming full correlation across the entire structure. This approximation is adopted, instead of a more rigorous random field approach [such as that suggested by Lee and Mosalam (2004)], to (1) reduce the computational cost associated with the potentially large number of RVs obtained from a proper discretization of the corresponding random fields; (2) simplify the physical interpretation of the probabilistic response results; and (3) avoid difficulties caused by the lack of data associated with the correlation lengths of the pertinent random fields. It is noted here that the assumption of full correlation within the entire structure for each random model parameter corresponds to assuming that the correlation length for the corresponding random field is larger than the dimension of the structural system considered. Although this assumption is not exact, it is known that the dispersion of the response parameters of a stochastic FE model is higher when the spatial variability of the model parameters is neglected (Lee and Mosalam 2004). Thus, the results obtained in this paper in terms of the dispersion of the EDPs can be considered as upper bounds of their actual dispersions.

The probability distributions and correlations between couples of model parameters adopted in this study are based on data reported in the literature, when available, or on engineering judgment, when sufficient data are not available. It is noteworthy

that a previous study (Barbato et al. 2010) showed that the correlation between couples of model parameters can affect, sometimes even significantly, the dispersion of the response parameters, particularly for highly nonlinear structural behavior. Thus, there is a clear need for more accurate and reliable estimates of the correlation coefficients between couples of model parameters. However, the accurate determination of these correlation coefficients is outside the scope of this paper. The joint probability density function (for all random parameters considered) required to generate the samples is obtained by using the Nataf model (Ditlevsen and Madsen 1996). A set of $N_{\text{sim}}$ samples of nonlinear FE structural models are obtained employing the Latin hypercube sampling (LHS) technique, as described in Iman and Conover (1982), where an efficient algorithm is also used to induce the target correlation between the variables. This algorithm is based on an iterative procedure that minimizes the scatter between the target and the sample correlation obtained for the generated sets of parameters.

The elastic and postelastic behavior of the structure is characterized on the basis of the moment–curvature ($M$–$\varphi$) response of the critical cross sections (CALTRANS 2006). Here, Monte Carlo simulation with LHS (Imam and Conover 1982) is coupled with $M$–$\varphi$ analysis to build probabilistic $M$–$\varphi$ curves (Tabsh 1996; Lee and Mosalam 2006) for the cross sections that most influence the bridge's transverse structural response. These cross sections are located at the base of the piers (which are expected to yield and may fail by reaching the ultimate curvature limit) and at the midspan of the deck (which is the deck cross-section most prone to yielding) (Tubaldi et al. 2010). Probabilistic $M$–$\varphi$ analysis is used to determine the statistical properties of stiffness and capacity of these structural components (i.e., deck and piers).

To separately identify the effects of randomness and uncertainty, both EIDA and IDA were performed. Multirecord IDA propagates the randomness-only effects to the EDPs. It entails generating $N_{\text{gm}}$ IDA curves based on a deterministic structural model corresponding to the mean/median values of the model parameters (referred to as the *basic structural model*). Multirecord EIDA involves the generation of $N_{\text{gm}} \cdot N_{\text{sim}}$ IDA curves reflecting the effects of both randomness and uncertainty. Both EIDA and IDA require the selection of an appropriate (i.e., efficient and sufficient) intensity measure (*IM*) (Shome et al. 1998) for scaling the ground motions to different intensity levels. *IM* selection is an important task in the probabilistic response and vulnerability analysis of structural systems subjected to seismic hazards. Efficiency of the *IM* ensures that good confidence in the results is achieved with a small number of analyses. Sufficiency of the *IM* ensures that the response is conditionally independent of the magnitude and source-to-site distance of the input ground motions. The spectral acceleration $S_a(\bar{T},\xi)$ at the fundamental period $\bar{T}$ of the structure for a given damping ratio $\xi$ has been recognized to be both efficient and sufficient for first mode-dominated systems. Thus, $S_a(\bar{T},\xi)$ is often preferred over other less efficient *IM*s, for example, peak ground acceleration (Shome et al. 1998). However, the choice of $S_a(\bar{T},\xi)$ as *IM* for uncertain structures (i.e., when uncertainty influences the value of the fundamental period of the structure) is not as straightforward as for deterministic structures. In this study, the $S_a(\bar{T},2\%)$ corresponding to the fundamental period of the basic structural model is assumed as the *IM* in both IDA and EIDA, consistent with the ground motion selection and modification (GMSM) method presented in Shome et al. (1998). It is noteworthy that the GMSM method used in this paper presents some limitations (PEER 2009; Katsanos et al. 2010). However, an in-depth analysis of these limitations is out of the scope of this paper.

The EDPs chosen in this study are the curvature demand at the base of the piers and the transverse curvature demand at the deck midspan. These EDPs are related to the two more important collapse modalities for SCC bridges with dual load path. Once EIDA and IDA curves are generated, the EDP statistics are estimated for different values of the *IM*. The influence of uncertainty on the probabilistic response of the bridge is evaluated based on the comparison between the median values and the dispersions of the EDPs according to EIDA and IDA for the discrete values of the *IM*. In particular, the response statistics considered are the 50th, 16th, and 84th fractiles of the EDPs. A quantitative measure of EDP dispersion is provided by the parameter $\beta$, defined as one-half of the natural logarithm of the ratio between the 84th and 16th fractiles of each monitored EDP at each *IM* value. It is noteworthy that, under the assumption of lognormality of the statistical distribution of the EDPs for a given value of *IM*, the parameter $\beta$ coincides with the estimate of the lognormal standard deviation of the EDP of interest. The median values of the EDPs resulting from EIDA are compared with the corresponding values obtained using IDA to evaluate the bias in the median response resulting from model parameter uncertainty. The dispersion of the EDPs resulting from both randomness and uncertainty, $\beta_{RU}$ (from EIDA); randomness only, $\beta_R$ (from IDA); and uncertainty only, $\beta_U$, are evaluated and compared to assess the influence of uncertainty on the response variability. The dispersion $\beta_U$ is computed as the average of the dispersions resulting from FE model variability obtained for each of the $N_{\text{gm}}$ ground motions considered (Dolsek 2009).

The influence of uncertainty on the fragility of the bridges investigated, assuming as limit states the exceedance of the curvature capacity of piers and deck. Failure in shear of the piers and abutment failure are ignored, assuming that a capacity design approach was used and that the probability of failure associated with these failure conditions is negligible. The statistical model of the capacity of piers and deck is obtained based on probabilistic $M$–$\varphi$ analysis, which is employed to propagate the uncertainty from model parameters to cross-section capacity. In this study, the component and system fragility curves are obtained through a numerical approach. It is noteworthy that the proposed methodology can be easily extended to include damage states other than those considered here. For example, the probabilistic moment–curvature curves can be employed to estimate the statistical distribution of the curvature corresponding to cover concrete cracking or spalling.

## Application Examples

### Description of the Basic Structural Models

The bridges considered in this paper have a total length of 130 m divided into three spans of lengths $L_1 = 40$ m, $L_2 = 50$ m, and $L_3 = 40$ m (Fig. 1). The superstructure is designed according to the specifications given in Eurocode 4 (ECS 2000) for the nonseismic load combinations (Dezi and Formica 2006). It consists of a 12-m-wide reinforced concrete slab, which can host two traffic lanes, and two steel girders positioned symmetrically with respect to the deck centerline at a distance of 6 m between their centerlines. Fig. 2(a) shows a typical cross section of the deck. The steel girders

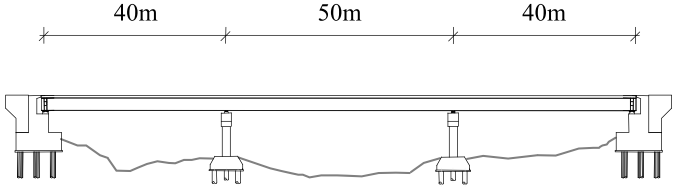


**Fig. 1.** Bridge longitudinal profile (slenderness ratio $H/D = 5$)

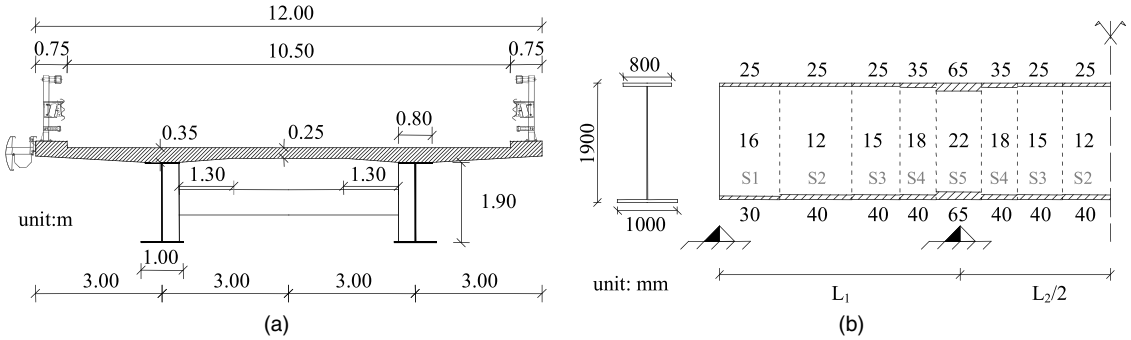


**Fig. 2.** Bridge deck cross section properties: (a) typical deck transverse cross section; (b) girder cross section geometry

are shown in Fig. 2(b), where the thicknesses of the flanges and web are provided for the five different girder cross sections (i.e., S1 through S5) used along the deck axis. The deck slab is haunched, and its thickness varies between 250 and 350 mm. The longitudinal reinforcement area is equal to 2% of the slab area at the supports (hogging regions) and 1% at midspans (sagging regions). The nominal distributed dead load due to self-weight of the structural and nonstructural elements permanently connected to the bridge is 138 kN/m (Dezi and Formica 2006). The deck is transversely fixed at the abutments. The reinforced concrete piers have a nominal circular cross section of diameter $D = 1.8$ m. Three different values of the slenderness are considered; that is, $H/D = 3$, 5, and 9, corresponding to height $H = 5.4$ m, 9.0 m, and 16.2 m. These values, selected on the basis of the parametric analysis performed in Tubaldi et al. (2010), describe three different types of seismic response. For the short piers, structural failure is due to excessive curvature in the piers. For the tall piers, structural failure is due to the deck yielding. The intermediate case is characterized by a "balanced failure." The piers have a constant longitudinal reinforcement steel ratio equal to 1%. Transverse reinforcement with a volumetric ratio $\rho_w = 0.5\%$ is provided in the hinge regions, with the goal of confining the concrete and preventing premature shear failure. Class C30/37 and C35/45 concrete is used for the piers and superstructure slab, respectively. The reinforcement bars are made of grade B450C steel, and the deck girders are made of grade S355 steel (ECS 2000). The bridge is assumed to rest on stiff soil, and the supports at the piers and abutments are modeled as rigid. Soil–structure interaction is not modeled, as it has negligible influence on the bridge's transverse seismic response for the bridge geometry and soil type considered (Tubaldi et al. 2010).

Dynamic nonlinear FE analyses of the bridges are performed using OpenSees (McKenna et al. 2006). The piers are modeled using the frame-with-hinges element developed by Scott and Fenves (2006), which is based on fiber-section integration over a specified hinge length, $L_p$, located at the pier base. The deck is modeled using linear elastic three-dimensional Timoshenko frame elements. Effective stiffness values are assigned to the deck and the elastic portion of the piers to account for concrete cracking.

### Ground Motion Uncertainty

A set of $N_{gm} = 18$ ground motion records is selected from the PEER (2006) database. These records refer to sites characterized by shear wave velocity $V_s$ higher than 800 m/s (stiff soil), with magnitudes in the range between 5.5 and 7.5 and source-to-site distance between 25 and 75 km. In Fig. 3(a) are plotted the pseudo-acceleration spectra of the selected ground motions (gray thin lines) and the corresponding mean spectrum (black thick line). In Fig. 3(b), the dispersion $\beta$ of the normalized spectra is plotted the period of vibration $T$ for the three models analyzed. It is observed that $\beta$ equals zero for the fundamental period of vibrations $\bar{T}$ in the transverse direction and assumes relatively high values (almost up to 1) for other periods.

### Model Parameter Uncertainty

The sources of uncertainty considered in this study are: (1) geometry, (2) material properties, (3) mass and dead loads, and (4) other parameters used to numerically model the structural behavior at the component and structure levels. Table 1 summarizes the model parameters' statistical information.

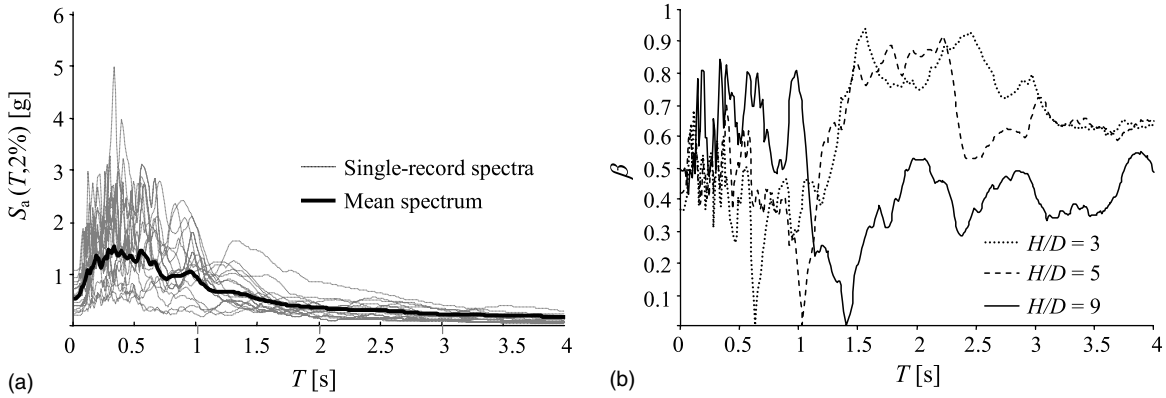


**Fig. 3.** Seismic ground motion uncertainty: (a) pseudo-acceleration spectra of the selected earthquake records and corresponding mean spectrum; (b) dispersion of the normalized spectra for the different models

**Table 1.** Statistical Description of Model Parameters

| RV | Description | Distribution | Mean | COV [%] |
|---|---|---|---|---|
| $D_p$ [m] | Section diameter | Normal | 1.8 | 0.55 |
| $c_d - c_r$ [mm] | Pier cover | Normal | 0 | ($\sigma = 0.01$) |
| $\varepsilon_{c,\text{core}}$ | Pier core concrete properties | Lognormal | 0.004 | 20 |
| $f_{c,\text{core}}$ [MPa] | | Lognormal | 45.75 | 20 |
| $\varepsilon_{cu,\text{core}}$ | | Lognormal | 0.0096 | 35 |
| $f_{cu,\text{core}}$ [MPa] | | Lognormal | 38.8 | 20 |
| $\varepsilon_{c,\text{cover}}$ | Pier cover concrete properties | Lognormal | 0.002 | 20 |
| $f_{c,\text{cover}}$ [MPa] | | Lognormal | 38 | 18.6 |
| $\varepsilon_{cu,\text{cover}}$ | | Lognormal | 0.0035 | 20 |
| $\varepsilon_{c,\text{deck}}$ | Deck slab concrete properties | Lognormal | 0.002 | 20 |
| $f_{c,\text{deck}}$ [MPa] | | Lognormal | 43 | 18.6 |
| $\varepsilon_{c,\text{deck}}$ | | Lognormal | 0.0035 | 20 |
| $f_{ys,\text{reinf}}$ [MPa] | Pier and deck slab reinforcement steel properties | Lognormal | 517.5 | 5.8 |
| $E_{s,\text{reinf}}$ [MPa] | | Lognormal | 201,000 | 3.3 |
| $f_{su,\text{reinf}}$ [MPa] | | Lognormal | 648 | 6.2 |
| $\varepsilon_{su,\text{reinf}}$ | | Lognormal | 0.09 | 8 |
| $\varepsilon_{su,bb}$ | | Lognormal | 0.062 | 25.4 |
| $f_{ys,\text{girder}}$ [MPa] | Deck girder steel properties | Normal | 419.38 | 5 |
| $E_{s,\text{girder}}$ [MPa] | | Normal | 209,000 | 6 |
| $W_{\text{sup}}$ [kN/m] | Superstructure weight | Normal | 143.3 | 8 |
| $W_{\text{sub}}$ [kN/m] | Substructure weight | Normal | 66.8 | 7 |
| $\xi$ | Global damping ratio | Lognormal | 0.02 | 30 |
| $L_p$ [m] | Plastic hinge length | Lognormal | 1.283 | 20 |

Regarding geometry, the section diameter, $D_p$, and the concrete cover, $c$, are modeled as RVs. The uncertainty of the latter is modeled by assigning a normal statistical distribution to the difference between the real in situ value, $c_r$, and the nominal (design) value, $c_d$. The statistical distributions of $c_d - c_r$ and $D_p$ are based on the Joint Committee on Structural Safety (JCSS) recommendations (JCSS 2000).

With respect to material properties, proper statistical distributions are assigned to the material parameters needed to define the constitutive models adopted (i.e., the constitutive parameters). Confined (the piers' core) and unconfined (the piers' cover and deck slab) concrete materials are both modeled via a Kent–Scott–Park (Kent and Park 1971) stress–strain model. The constitutive parameters assumed as uncertain for the unconfined concrete of the piers' cover (class 30/37) and the deck slab (class 40/45) are: (1) peak strength, $f_{c,\text{cover}}$ and $f_{c,\text{deck}}$; (2) strain at peak strength, $\varepsilon_{c,\text{cover}}$ and $\varepsilon_{c,\text{deck}}$; and (3) strain at rupture, $\varepsilon_{cu,\text{cover}}$ and $\varepsilon_{cu,\text{deck}}$. The residual stress for strain larger than $\varepsilon_{cu,\text{cover}}$ is assumed deterministically to be zero. The statistical distribution of the peak strength is taken from Barlett and McGregor (1996), and the distribution of the ultimate strain is taken from Barbato et al. (2010) and is characterized by a coefficient of variation (COV) of 20%. The effect of confinement on the concrete core in the piers' plastic hinge zones is based on Mander's model (Mander et al. 1988). The constitutive parameters modeled as RVs for the confined concrete are: (1) peak strength, $f_{c,\text{core}}$; (2) strain at peak strength, $\varepsilon_{c,\text{core}}$; (3) strength at rupture, $f_{cu,\text{core}}$; and (4) strain at rupture, $\varepsilon_{cu,\text{core}}$. The COV of $\varepsilon_{cu,\text{core}}$ is based on the work of Kappos et al. (1999).

The Menegotto–Pinto model (Menegotto and Pinto 1973) is used to characterize the reinforcement steel behavior. The following constitutive parameters are assumed as RVs: (1) yield stress, $f_{sy,\text{reinf}}$; (2) elastic modulus, $E_{s,\text{reinf}}$; (3) ultimate stress, $f_{su,\text{reinf}}$; and (4) ultimate strain $\varepsilon_{su,\text{reinf}}$. An additional RV is introduced to account for longitudinal bar buckling. According to Berry (2006), longitudinal bar buckling takes place when the absolute value of the compressive strain of the steel reinforcement is larger than the limit value

$$\varepsilon_{su,bb} = \chi_1 + \chi_2 \cdot \rho_{\text{eff}} \tag{1}$$

where $\rho_{\text{eff}} = \rho_s \cdot f_{ys}/f_c$ = effective confinement ratio, with $\rho_s$ = transverse reinforcement ratio, $f_{ys}$ = yield stress of transverse reinforcement, and $f_c$ = concrete compressive strength; and $\chi_1 = 0.045$ and $\chi_2 = 0.25$ are constants calibrated on experimental results. The mean value of $\varepsilon_{su,bb}$ for the case examined here is 0.062, and the COV is 25.4%. The statistical description of the parameters defining the girder steel stress–strain relation is obtained from the literature (JCSS 2000; Da Silva et al. 2009). The elastic modulus of the girder steel, $E_{s,\text{girder}}$, has a mean value of 209,000 MPa and a COV of 6%. The influence of plate thickness on the definition of the yield stress of the girder steel, $f_{ys,\text{girder}}$, is not considered here. However, it is noteworthy that the complete girder steel stress–strain relation is needed for the probabilistic $M$–$\varphi$ analysis.

The structure self-weight is characterized by moderate uncertainty because of variations in material densities, member sizes, and overlay thickness (Nowak and Szerszen 1998). The following components of dead loads are considered: (1) weight of factory-made elements (steel, precast concrete members); (2) weight of cast-in-place concrete members; (3) weight of the wearing surface (asphalt); and (4) miscellaneous weights (e.g., pipes, luminaries). Dead loads are modeled by two normal RVs corresponding to loads acting on the superstructure, $W_{\text{sup}}$, and on the substructure, $W_{\text{sub}}$.

The sources of uncertainty characterizing the structural behavior include: (1) modal damping ratio, $\xi$, and (2) plastic hinge length, $L_p$, in the piers. The modal damping ratio is assumed to follow a lognormal distribution with mean equal to 0.02 and a COV of 30%. The modal damping ratio is used to build a Rayleigh-type FE damping matrix (McKenna et al. 2006), based on the periods of

vibration of the two modes with the highest participating mass in the transverse direction. The variability of these periods caused by uncertainty is taken into account by performing modal analysis on the sample models. The plastic hinge length, $L_p$, has a lognormal distribution, with the mean value obtained following Eurocode 8 (ECS 2005) and a COV of 20% (Lupoi et al. 2003; Lessloss-Risk 2007).

In this study, the correlation coefficients $\rho$ between couples of parameters describing the confined and unconfined concrete are assumed as follows: $\rho = 0.8$ for (1) $f_{c,\text{core}}$ and $f_{cu,\text{core}}$, (2) $\varepsilon_{c,\text{core}}$ and $\varepsilon_{cu,\text{core}}$, (3) $\varepsilon_{c,\text{cover}}$ and $\varepsilon_{cu,\text{cover}}$, (4) $f_{c,\text{core}}$ and $f_{c,\text{cover}}$, (5) $\varepsilon_{c,\text{core}}$ and $\varepsilon_{c,\text{cover}}$, (6) $\varepsilon_{cu,\text{core}}$ and $\varepsilon_{cu,\text{cover}}$, and (7) $\varepsilon_{c,\text{deck}}$ and $\varepsilon_{cu,\text{deck}}$; $\rho = 0.64$ for (1) $f_{cu,\text{core}}$ and $f_{c,\text{cover}}$, (2) $\varepsilon_{c,\text{core}}$ and $\varepsilon_{cu,\text{cover}}$, and (3) $\varepsilon_{cu,\text{core}}$ and $\varepsilon_{c,\text{cover}}$; and $\rho = 0.0$ for all other pairs of parameters (Barbato et al. 2010). The correlation coefficients between the reinforcement steel parameters are $\rho = 0.85$ for $f_{ys,\text{reinf}}$ and $f_{su,\text{reinf}}$, $\rho = -0.5$ for $f_{ys,\text{reinf}}$ and $\varepsilon_{su,\text{reinf}}$, and $\rho = -0.55$ for $f_{su,\text{reinf}}$ and $\varepsilon_{su,\text{reinf}}$ (JCSS 2000). A correlation coefficient $\rho = 0.5$ between $D_p$ and $c_d - c_r$ is assumed based on engineering judgment. Constitutive parameters from different materials are assumed to be uncorrelated.

In addition to the variables listed in Table 1, the effective stiffness and curvature capacity of piers and deck are modeled as RVs. Their statistical distributions are based on probabilistic $M$–$\varphi$ analysis.

### Probabilistic Structural Finite-Element Model

$N_{\text{sim}} = 50$ samples of $N = 24$ model parameters are generated using the LHS technique and the joint probability distribution of the model parameters obtained through the Nataf model. $N_{\text{sim}}$ is chosen to ensure a good match between target and sample statistical distributions and correlation matrix. It is observed that $N_{\text{sim}}$ used here is higher than the value $N$ suggested in Dolsek (2009). A FE model of each bridge under study is built for each generated sample of model parameters. Probabilistic $M$–$\varphi$ analysis of the deck midspan section and the piers' base sections is performed based on the assumed joint probability distribution of the model parameters. Table 2 provides the probabilistic $M$–$\varphi$ analysis results in terms of the statistics of the parameters describing the behavior of the cross sections of interest.

The probabilistic $M$–$\varphi$ curves for the piers' base cross sections are determined for a constant value of the axial force equal to the mean value of the axial force induced by the permanent loads acting on the bridge corresponding to $H/D = 5$. This assumption is deemed appropriate in this study because the changes in the axial force during the seismic action have a negligible influence on the cross section behavior of the structural system analyzed (Tubaldi et al. 2010), when only the transverse component of the seismic input is considered. However, it is worth mentioning that this assumption may not be valid in other cases where the vertical component of seismic input significantly affects the piers' seismic response. The probabilistic $M$–$\varphi$ analysis for the piers' base cross sections provides the statistics for the yield and ultimate values of the curvature and moment. The yield point $(M_{y,p}, \varphi_{y,p})$ corresponds to the yielding of the longitudinal bars. The ultimate conditions $(M_{u,p}, \varphi_{u,p})$ are attained either when the confined concrete fails or when steel reinforcement reaches the limit tensile strain or the bucking strain. For each sample of model parameters, an effective stiffness, $EI_{\text{eff},p}$, is obtained as the ratio between $M_{y,p}$ and $\varphi_{y,p}$. In addition to the model parameters listed in Table 1, the $N_{\text{sim}}$ values of $EI_{\text{eff},p}$ obtained from the probabilistic $M$–$\varphi$ analyses are employed to define the elastic portion of the beam-with-hinges elements of the FE models used in the time-history analyses. The corresponding $N_{\text{sim}}$ values of $\varphi_{u,p}$ are used to define the capacity of the piers in the vulnerability assessment. It is observed that $\varphi_{u,p}$ is (1) highly correlated ($\rho > 0.8$) with core ($\varepsilon_{cu,\text{core}}$) and cover ($\varepsilon_{cu,\text{cover}}$) concrete ultimate deformations; (2) moderately correlated ($0.6 < \rho < 0.8$) with core ($\varepsilon_{c,\text{core}}$) and cover ($\varepsilon_{c,\text{cover}}$) concrete peak deformations; and (3) lowly correlated ($\rho < 0.35$) with strength-related parameters of the concrete materials (i.e., $f_{c,\text{core}}$, $f_{c,\text{cover}}$, $f_{cu,\text{core}}$). It is also found that $EI_{\text{eff},p}$ is (1) highly correlated with $f_{c,\text{core}}$; (2) moderately correlated with $f_{c,\text{cover}}$ and $f_{cu,\text{core}}$; and (3) inversely correlated with $\varepsilon_{c,\text{core}}$ ($\rho = -0.53$) and $\varepsilon_{c,\text{cover}}$ ($\rho = -0.43$).

The probabilistic $M$–$\varphi$ analysis for the midspan cross section of the central span provides the statistics for the transverse effective stiffness, $EI_{\text{eff},d}$, and the curvature capacity of the superstructure, $\varphi_{y,d}$. According to a previous parametric study (Tubaldi et al. 2010), failure of the superstructure is most likely to be reached at the midspan of the longest span. The values of $EI_{\text{eff},d}$ and $\varphi_{y,d}$ of other deck cross sections are assumed to follow the same distribution as that identified for the midspan section. The value of $EI_{\text{eff},d}$, which accounts for slab cracking induced by the transverse seismic forces, is defined as the ratio of yield moment, $M_{y,d}$, to yield curvature, $\varphi_{y,d}$, determined via probabilistic $M$–$\varphi$ analysis. The yielding condition is defined by Eurocode 8 (ECS 2005). It is observed that $EI_{\text{eff},d}$ is highly correlated with $f_{c,\text{deck}}$ and $E_{s,\text{girder}}$, whereas $\varphi_{y,d}$ is highly positively correlated with $f_{ys,\text{reinf}}$ and slightly negatively correlated with $f_{c,\text{deck}}$ and $E_{s,\text{reinf}}$.

**Table 2.** Probabilistic Moment–Curvature Analysis Results

| RV | Description | mean | COV [%] |
|---|---|---|---|
| $\varphi_{y,p}$ [1/m] | Pier yield curvature | 0.0023 | 7.72 |
| $M_{y,p}$ [kN-m] | Pier yield moment | 11,304 | 4.73 |
| $\varphi_{u,p}$ [1/m] | Pier ultimate curvature | 0.02617 | 37.8 |
| $M_{u,p}$ [kN-m] | Pier ultimate moment | 15,351 | 5.27 |
| $EI_{\text{eff},p}$ [kN-m$^2$] | Pier effective stiffness | 4.91E + 06 | 8.53 |
| $\varphi_{y,d}$ [1/m] | Deck yield curvature | 0.00039 | 7.96 |
| $M_{y,d}$ [kN-m] | Deck yield moment | 206,000 | 7.13 |
| $EI_{\text{eff},d}$ [kN-m$^2$] | Deck effective stiffness | 6.09$E$ + 08 | 5.66 |

## Statistical Analysis of the Structural Response

In this section, the statistics of the EDPs obtained from EIDAs (accounting for both randomness and uncertainty) and IDAs (accounting only for randomness) are illustrated and compared to gain insight into the contribution (jointly and separately) of randomness and uncertainty to the variability of EDPs. In this application, the FE time-history analyses (49500 for EIDA, 990 for IDA) were performed using parallel computation on a computer cluster comprising 104 central processing units (Tubaldi et al. 2010). For the three bridges considered, Fig. 4 plots the 16th, 50th, and 84th fractile curves of the piers' curvature [Figs. 4(a), 4(c), and 4(e)] and the deck's midspan transverse curvature [Figs. 4(b), 4(d), and 4(f)] for a given $IM$, obtained from both IDAs ($R$) and EIDAs ($RU$). The response of the models corresponding to $H/D = 3$ and $H/D = 5$ is significantly nonlinear and results in the piers experiencing large inelastic deformations. The deck curvature demand is most important in the models corresponding to $H/D = 5$ and $H/D = 9$. The median curvature demand evaluated for the basic structural models, which reflects randomness effects only ($R$), is very close to the median curvature demand estimated including model parameter uncertainty effects ($RU$) (i.e., the median seismic response of the bridges considered is almost independent of uncertainty $U$).

The relative importance of the various sources of uncertainty can be studied by comparing the dispersion $\beta_{RU}$ caused by both

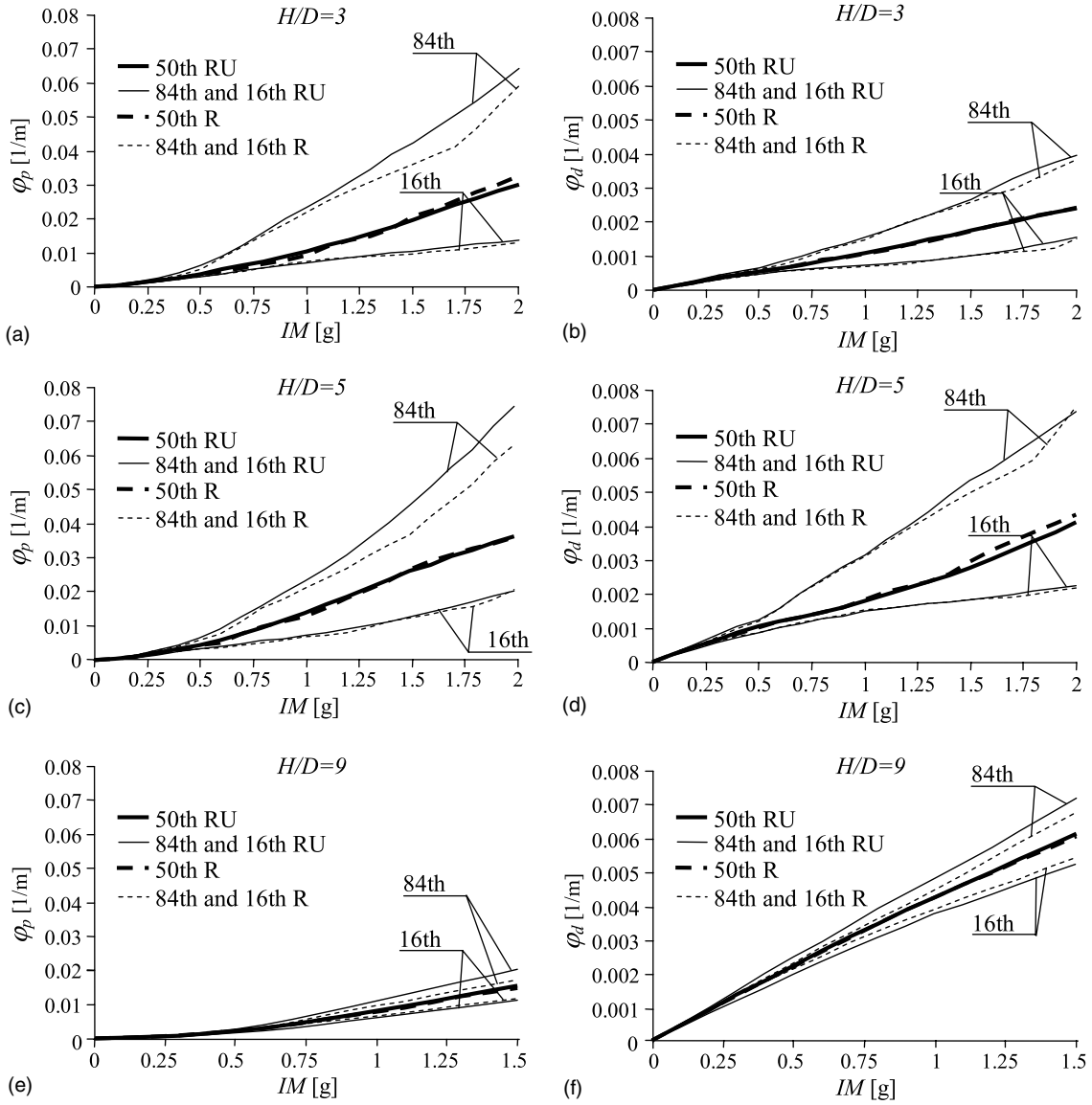


**Fig. 4.** Curvature demand versus seismic intensity *IM*: (a) piers' curvature demand $\varphi_p$ for piers' slenderness ratio $H/D = 3$; (b) deck's midspan transverse curvature demand $\varphi_d$ for $H/D = 3$; (c) $\varphi_p$ for $H/D = 5$; (d) $\varphi_d$ for $H/D = 5$; (e) $\varphi_p$ for $H/D = 9$; (f) $\varphi_d$ for $H/D = 9$

randomness $R$ and uncertainty $U$ with the dispersion $\beta_R$ caused by ground motion uncertainty only and the dispersion $\beta_U$ caused by uncertainty only. Fig. 5 shows the dispersion measures for the piers' and deck's curvature demand as functions of the *IM*, in which $H/D = 3$, 5, and 9. It is observed from Fig. 5 that, for all EDPs considered, the dispersion measure $\beta_U$ is only slightly influenced by *IM* values and by bridge global behavior (i.e., $H/D$ ratio). The dispersion $\beta_U$ of the piers' curvature demand attains a maximum value of 0.35 for low *IM* values, whereas it remains almost constant and equal to about 0.23 for a wide range of *IM* values, for all $H/D$ values considered. Dispersion $\beta_U$ of the deck's curvature demand assumes smaller values, in the range 0.10–0.15 for a wide range of *IM* values, in all models considered.

Dispersion $\beta_R$ related to ground motion randomness generally increases as *IM* increases, for all EDPs considered. Dispersion $\beta_R$ of the piers' curvature demand is higher than that of the deck's curvature demand, for all *IM* values considered. The values of $\beta_R$ for both EPDs are significantly higher for $H/D = 3$ and $H/D = 5$ than for $H/D = 9$. This is a consequence of the high efficiency of the *IM* used here in the case of slender piers, which exhibit an almost elastic response up to high *IM* values.

Evaluation of the dispersion $\beta_{RU}$ for any EDP involves performing a significantly large number of FE simulations and, thus, is computationally expensive. Therefore, for practical applications, it is of interest to develop an approximate technique for estimating $\beta_{RU}$ at lower computational cost. On the basis of the observation that $\beta_U$ is almost constant for different values of *IM*, an approximate estimate of the dispersion $\beta_{RU}$, referred to as $\beta_{SRSS}$, is suggested here. This approximate expression is defined as the square root of sum of squares of $\beta_R$ and the constant asymptotic value, $\bar{\beta}_U$, of the dispersion $\beta_U$; that is, $\beta_{SRSS} = (\beta_R^2 + \bar{\beta}_U^2)^{1/2}$.

Fig. 5 compares $\beta_{SRSS}$ with $\beta_{RU}$, for both piers' curvature demand [Figs. 5(a), 5(c), and 5(e)] and deck's curvature demand (Figs. 5(b), 5(d), and 5(f)]. The difference between $\beta_{SRSS}$ and $\beta_{RU}$ for all EDPs investigated is very small, particularly for high *IM* values. Thus, a satisfactory estimation of $\beta_{RU}$ can be obtained through $\beta_{SRSS}$ by (1) performing multirecord IDAs using the basic structural model (i.e., by computing $\beta_R$), and (2) evaluating

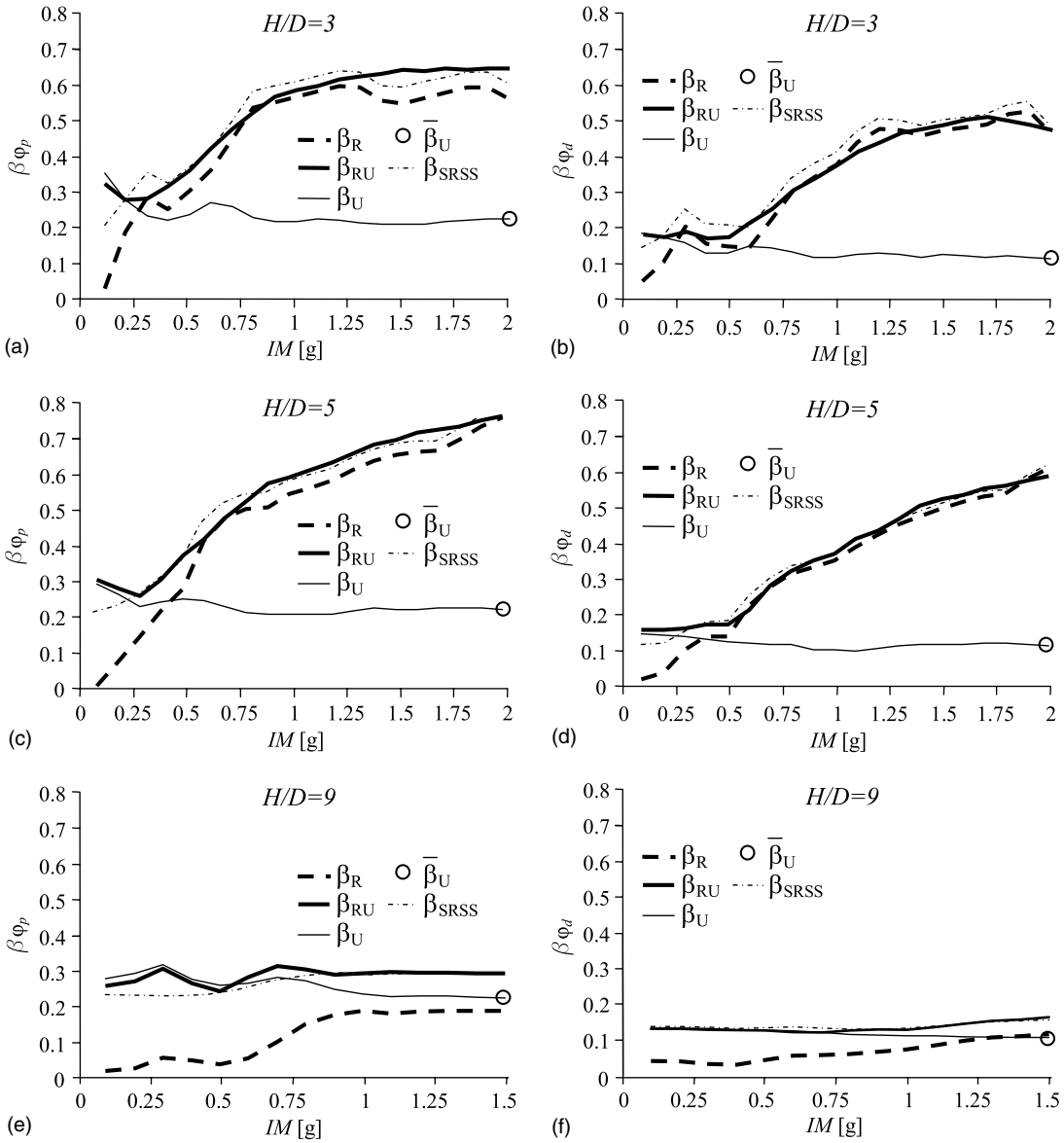


**Fig. 5.** Dispersion $\beta$ of curvature demand versus seismic intensity $IM$: (a) piers' curvature dispersion $\beta_{\varphi_p}$ for piers' slenderness ratio $H/D = 3$; (b) deck's midspan curvature dispersion $\beta_{\varphi_d}$ for $H/D = 3$; (c) $\beta_{\varphi_p}$ for $H/D = 5$; (d) $\beta_{\varphi_d}$ for $H/D = 5$; (e) $\beta_{\varphi_p}$ for $H/D = 9$; and (f) $\beta_{\varphi_d}$ for $H/D = 9$

$\bar{\beta}_U$ through Monte Carlo analysis for only a single $IM$ value (e.g., the $IM$ value dominating the hazard of the site). Further reduction of computational cost, although not investigated in the present study, could be achieved by estimating $\bar{\beta}_U$ through less computationally demanding FE analyses, for example, probabilistic pushover analysis (Vamvatsikos and Fragiadakis 2010; Barbato et al. 2010).

To determine which parameters most influence the response of SCC bridges with dual load path, Spearman rank correlation coefficients, $\rho_{\text{inp-out}}$, between model parameters and EDPs (i.e., curvature demand at the piers' bases, $\varphi_p$, and at the deck midspan section, $\varphi_d$) are evaluated, and their dependence on $IM$ is analyzed. These coefficients (Saltelli et al. 2000) are nonparametric measures of statistical dependence between two variables and indicate the extent to which one variable tends to increase as the other variable increases. Therefore, they provide an indirect measure of the response sensitivity with respect to the model parameters. Because of space constraints, only selected results for the case $H/D = 5$ are shown in Fig. 6. It is observed that $\varphi_p$ presents a significant inverse correlation with the plastic hinge length, $L_p$, for high $IM$ values. In fact, $\varphi_p$ increases for decreasing $L_p$ because of localization effects. An inverse correlation is also observed between $\varphi_p$ and the damping coefficient ratio $\xi$, and between $\varphi_d$ and $\xi$. This

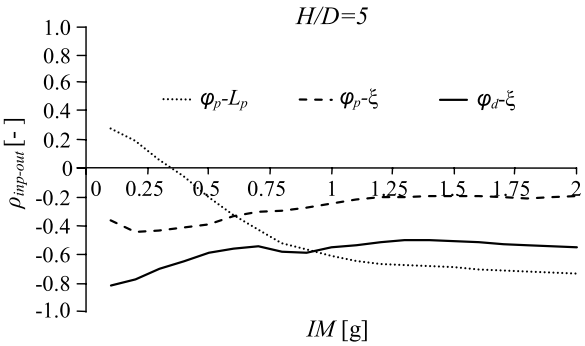


**Fig. 6.** Correlation coefficients $\rho_{\text{inp-out}}$ between input variables and EDPs for slenderness ratio $H/D = 5$

correlation decreases after the piers' yielding because the hysteretic dissipation at the plastic hinges becomes larger than the energy dissipation resulting from viscous damping. The correlation coefficients between the EDPs and the other input uncertainties are smaller (in absolute value) than 0.3 for all *IM* values considered. Similar results are observed also for the cases corresponding to $H/D = 3$ and $H/D = 9$. For $H/D = 3$, a positive correlation ($\rho_{\text{inp-out}} \approx 0.5$) is also observed between deck mass and $\varphi_d$. As expected, for $H/D = 9$, $\varphi_p$ is positively correlated with strain parameters $\varepsilon_{c,\text{core}}$, $\varepsilon_{cu,\text{core}}$, $\varepsilon_{c,\text{cover}}$, and $\varepsilon_{cu,\text{cover}}$, and negatively correlated with the strength parameters $f_{c,\text{core}}$, $f_{cu,\text{core}}$, and $f_{c,\text{cover}}$, for *IM* values smaller than the value corresponding to the yielding of the piers.

## Statistical Analysis of the Structural Fragility

This study presents the fragility curves for SCC bridges with dual load path characterized by different $H/D$ values. Fragility curves represent the probability that a specified limit state or failure condition is exceeded, conditional on the value of the *IM*. They are used here to identify the most probable failure mechanisms occurring in the different bridge configurations considered, and to characterize the probabilistic behavior at collapse. The failure conditions considered are flexural failure at the base of the piers ($\varphi_p \geq \varphi_{u,p}$) and yielding at the deck midspan ($\varphi_d \geq \varphi_{y,d}$). The approach followed in this study accounts explicitly for the correlation between structural demand and capacity through the use of probabilistic $M$–$\varphi$ analysis to define both the probabilistic FE model and capacity of the structure.

Fig. 7 plots the fragility curves corresponding to each of the two component limit states [Figs. 7(a), 7(c), and 7(e))] and to the global system failure [Figs. 7(b), 7(d), and 7(f)] for the different bridge configurations ($H/D = 3$, 5, and 9). Fig. 7 also compares results obtained from IDAs (dashed lines denoted as *R*) and from EIDAs (solid lines denoted as *RU*). For $H/D = 3$, the piers are the most fragile component, and the probability of deck yielding, $P_{F,d}$, is significantly smaller than the probability of the piers' flexural failure, $P_{F,p}$, at every *IM* value considered. For $H/D = 9$, the opposite behavior is observed, with $P_{F,d}$ significantly larger than $P_{F,p}$. Thus, for slender piers, the dissipation capacity of the piers cannot be

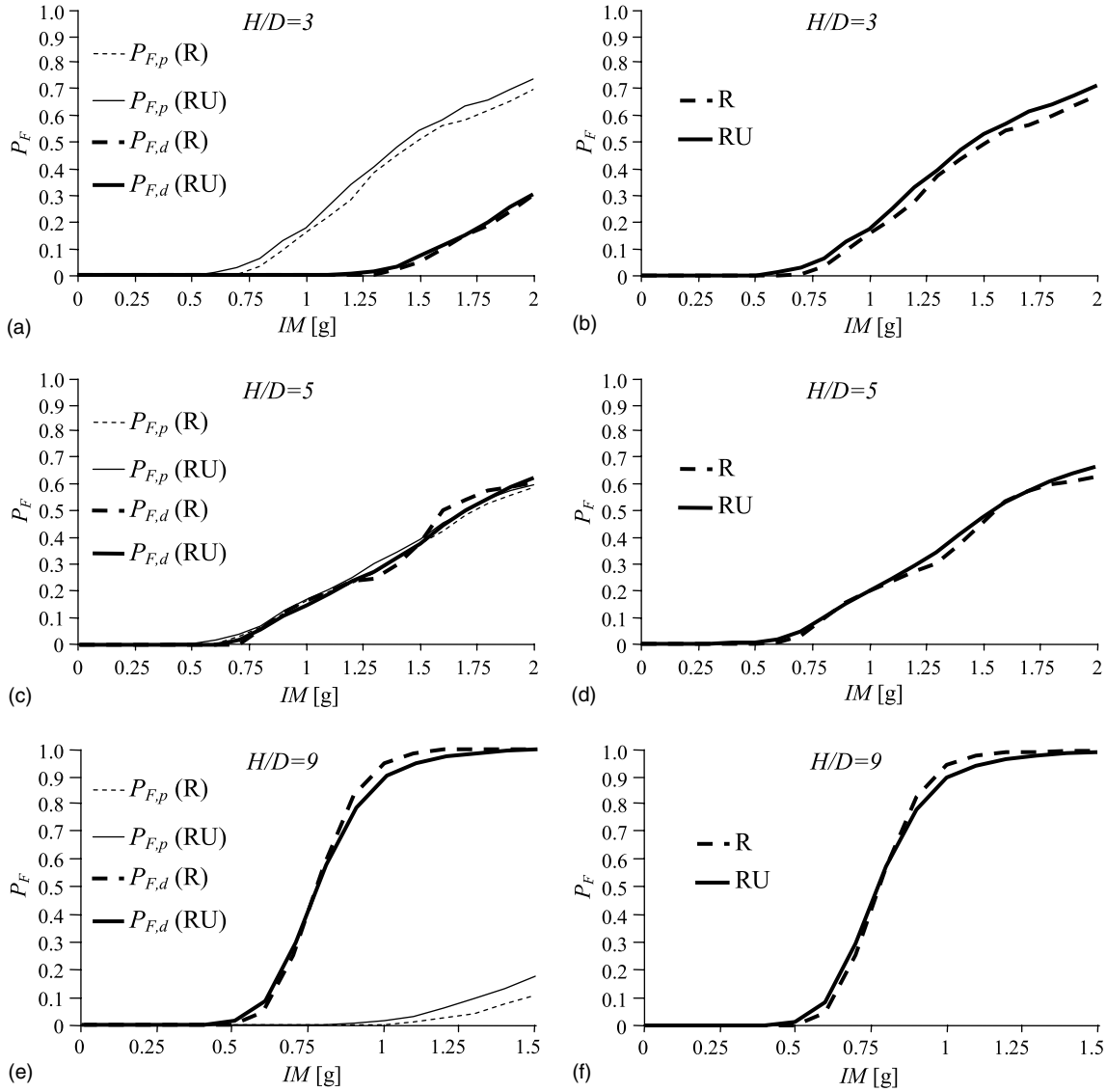


**Fig. 7.** Component (left) and system (right) fragility curves: (a) fragility curve relative to flexural failure of piers $P_{F,p}$ and deck's midspan $P_{F,d}$ for slenderness ratio $H/D = 3$; (b) system fragility curve $P_F$ for $H/D = 3$; (c) $P_{F,p}$ and $P_{F,d}$ for $H/D = 5$; (d) $P_F$ for $H/D = 5$; (e) $P_{F,p}$ and $P_{F,d}$ for $H/D = 9$; (f) $P_F$ for $H/D = 9$

completely exploited because of deck yielding. For $H/D = 5$, the probabilities of failure associated with the two component limit states are similar in magnitude, leading to a "balanced failure" of both components at every value of $IM$. It is observed that uncertainty has a small influence on the component fragilities. The effect of uncertainty is a small increase in the fragility of each component, except for $H/D = 9$ and large $IM$ values.

The system fragility curves in Figs. 7(b), 7(d), and 7(f) are obtained by accounting rigorously (through direct simulation) for the correlation between different failure modes. In general, model parameter uncertainty produces two effects on the system fragility curve: (1) an increase in the dispersion of the demand and, thus, a flattening of the fragility curves; and (2) a shift in the median value of the fragility (Liel et al. 2009). For $H/D = 3$ and 5, the values of $P_f$ conditioned on $IM$ obtained from EIDAs (i.e., including both randomness and uncertainty in evaluation of EDPs) are slightly higher than the values obtained from IDAs (i.e., including only randomness in evaluation of EDPs), which is consistent with results reported in other studies (Vamvatsikos and Fragiadakis 2010). For $H/D = 9$, the median value shift is negligible, and the fragility dispersion's increase is dominant. Thus, the fragility curve accounting for both randomness and uncertainty is flatter than the fragility curve accounting only for randomness. Assuming that the system fragility follows a lognormal distribution, the ratio of the lognormal standard deviation accounting for and disregarding uncertainty is about 1.25 in the case of slender piers. Thus, the effects of model parameter uncertainty on the bridges' seismic vulnerability are very significant.

In Fig. 8, the system fragility curve accounting for the exact correlation between failure modes for the bridge with $H/D = 5$ (i.e., with balanced failure) is compared with the system fragility curves obtained by approximate combination of the component fragilities by assuming full correlation or independence between the failure modes. It is observed that the correlation between the two considered failure modes is significant, and that the fragility curve obtained from direct simulation is contained and is almost equidistant from the two approximate fragility curves. For $H/D = 3$ and 9, the correlation between the considered failure modes, although present, has negligible effects on system fragility, as these bridges are characterized by a dominant failure mode. This observation can be used to reduce the computational cost of the vulnerability assessment procedure. In fact, for structures characterized by a dominant failure mode, the correlation between different failure modes can be ignored with negligible effects on the accuracy of the system failure probability estimate.

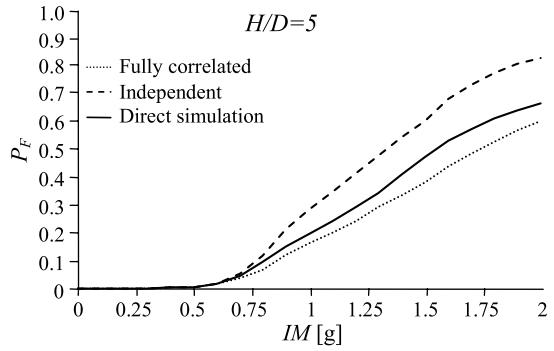


**Fig. 8.** Comparison of different estimates of the system fragility curve for slenderness ratio $H/D = 5$

## Conclusions

This paper investigates the seismic response and vulnerability of SCC bridges exhibiting dual load path. A fully probabilistic approach is proposed to account for both the seismic input uncertainty resulting from the record-to-record variability and the uncertainty affecting model parameters, such as geometric dimensions, material properties, mass, gravity loads, and dissipative properties.

The proposed methodology combines the LHS technique with a probabilistic moment–curvature analysis to build a lumped plasticity probabilistic FE model of SCC bridges with dual load path. This methodology allows for the building of FE models that are sufficiently accurate for real-world engineering applications, while containing the overall computational cost of the nonlinear FE time-history analysis. The aforementioned feature is crucial to ensure the feasibility of the proposed methodology, as accurate and reliable probabilistic response and vulnerability results usually require a significantly large number of nonlinear FE time-history analyses. The propagation of the uncertainty from the seismic input and model parameters to the seismic response is accomplished by means of EIDA, which is innovatively employed to perform seismic fragility analysis of bridge structures.

The proposed methodology is applied to a set of three-span continuous SCC bridges with transverse restraints at the abutments to evaluate the effects of model parameter uncertainty on seismic response and vulnerability, and to highlight critical problems in the design and assessment of SCC bridges with dual load path. Three different stiffness ratios between deck and piers (represented by the ratio $H/D$ between the piers' height $H$ and the piers' diameter $D$) are considered to examine the different seismic behavior and failure modes usually exhibited by these structures. Based on the results of the study performed in this paper, the following observations are made for SCC bridges with dual load path: (1) The effects on structural response variability of seismic ground motion uncertainty are significantly larger than the effects of model parameter uncertainty for $H/D = 3$ and $H/D = 5$ and smaller for $H/D = 9$. (2) Explicitly considering the model parameter uncertainty increases the dispersion of the simulated seismic response, as measured by the parameter $\beta$, defined as one-half of the logarithm of the ratio between the 84th and 16th percentiles of the EDP of interest. The dispersion caused by the model parameter uncertainty only, $\beta_U$, assumes not negligible values, which depend on the different EDPs considered. By contrast, this dispersion is almost independent of the values of the $IM$ and of the bridge behavior (described by the ratio $H/D$). The dispersion $\beta_U$ assumes larger values for the piers' curvature demand than for the deck's curvature demand. (3) The seismic response is very sensitive to the piers' plastic hinge length. Furthermore, for low values of $IM$, the values of the monitored EDPs are negatively correlated with structural damping. (4) The effects of model parameter uncertainty on system fragility are small but not negligible. (5) The correlation between different failure modes is significant only for the case in which a balanced failure is attained (i.e., $H/D = 5$ for the application example considered in this paper), whereas it is negligible in cases characterized by a dominant failure mode (i.e., $H/D = 3$ and 9).

The proposed methodology provides a rigorous tool to evaluate the effects of model parameter uncertainty on seismic response and fragility of various structural systems. In fact, although the results presented in this study are limited to SCC bridges with dual load path, this rigorous methodology can be readily applied to different bridge and structural typologies. Parametric studies similar to that presented here can provide important information on the relative importance of different sources of uncertainty for a variety of structures. This methodology can also provide benchmark results

needed to develop more efficient computational tools, which can be used to estimate the effects of model parameter uncertainty on the seismic response and fragility of a wide range of structural systems.

On the basis of the results obtained using the presented rigorous procedure, a simplified procedure is proposed to estimate the dispersion of the monitored EDPs including explicitly the effects of model parameter uncertainty. This simplified procedure combines classic IDA with Monte Carlo analysis performed for only one value of the seismic intensity. It is shown that, for the benchmark problems considered, the simplified procedure provides sufficiently accurate results at a fraction of the computational cost of the rigorous procedure.

## Acknowledgments

The authors gratefully acknowledge partial support of this research by the Louisiana Board of Regents through (1) the Pilot Funding for New Research Program of the National Science Foundation Experimental Program to Stimulate Competitive Research under Award No. NSF(2008)-PFUND-86, and (2) the Research & Development Program, Research Competitiveness Subprogram, under Award No. LEOSF(2010-13)-RD-A-01. Opinions expressed in this study are those of the authors and do not necessarily reflect those of the sponsor.

## References

Astaneh-Asl, A., Bolt, B., Mcmullin, K. M., Donikian, R. R., Modjtahedi, D., and Cho, S. W. (1994). "Seismic performance of steel bridges during the 1994 Northridge earthquake." *Report No. UCB/CE-Steel-94/01*, Dept. of Civil Engineering, Univ. of California, Berkeley.

Barbato, M., Gu, Q., and Conte, J. P. (2010). "Probabilistic push-over analysis of structural and soil–structure systems." *J. Struct. Eng.*, 136(11), 1330–1341.

Barlett, F. M., and MacGregor, J. G. (1996). "Statistical analysis of the compressive strength of concrete in structures." *ACI Mater. J.*, 93(2), 158–168.

Berry, M. P. (2006). "Performance modeling strategies for modern reinforced concrete bridge columns." Ph.D. dissertation, Univ. of Washington.

California Department of Transportation (CALTRANS). (2006). Seismic Design Criteria 1.4, Sacramento, CA.

Calvi, G. M. (2004). "Recent experience and innovative approaches in design and assessment of bridges." *Proc., 13th World Conference on Earthquake Engineering*, Vancouver, Canada, August 1–6, 2004, Paper No. 5009.

Collings, D. (2005). *Steel–Concrete Composite Bridges*, Thomas Telford, London.

Da Silva, L. S., Rebelo, C., Nethercot, D., Marques, L., Simões, R., and Vila Real, P. M. M. (2009). "Statistical evaluation of the lateral–torsional buckling resistance of steel I-beams, Part 1: Variability of steel properties." *J. Constr. Steel Res.*, 65(4), 832–849.

Dezi, L., and Formica, M. (2006). "Impalcato bitrave a sezione composta. Verifica secondo gli eurocodici." *Strutture Composte: Nuove Costruzioni, Recupero, Ponti*, CISM, Italy (in Italian).

Ditlevsen, O., and Madsen, H. O. (1996). *Structural Reliability Methods*, Wiley, New York.

Dolsek, M. (2009). "Incremental dynamic analysis with consideration of modeling uncertainties." *Earthquake Eng. Struct. Dyn.*, 38(6), 805–825.

Dymiotis, C., Kappos, A. J., and Chryssanthopoulos, M. K. (1999). "Seismic reliability of RC frames with uncertain drift and member capacity." *J. Struct. Eng.*, 125(9), 1038–1047.

European Committee for Standardization (ECS). (2000). *Eurocode 4. Design of composite steel and concrete structures. Part 2: Composite bridges*, *ENV 1994-2*, Brussels.

European Committee for Standardization (ECS). (2005). *Eurocode 8. Design of structures for earthquake resistance. Part 2: Bridges*, *EN 1998*, Brussels.

Federation Internationale du Beton (FIB). (2007). "*Seismic bridge design and retrofit—structural solutions*." FIB Bulletin 39, Lausanne, Switzerland.

Hwang, H. H. M., and Jaw, J. W. (1990). "Probabilistic damage analysis of structures." *J. Struct. Eng.*, 116(7), 1992–2007.

Iman, R. L., and Conover, W. J. (1982). "A distribution-free approach to inducing rank correlation among input variables." *Commun. Statist. Part B, Simul. Comput.*, 11(3), 311–334.

Itani, A. M., Bruneau, M., Carden, L. P., and Buckle, I. G. (2004). "Seismic behavior of steel girder bridge superstructures." *J. Bridge Eng.*, 9(3), 243–249.

Joint Committee on Structural Safety (JCSS). (2000). Probabilistic Model Code, 12th draft, Lyngby, Denmark.

Kappos, A. J., Chryssanthopoulos, M. C., and Dymiotis, C. (1999). "Uncertainty analysis of strength and ductility of confined reinforced concrete members." *Eng. Struct.*, 21(3), 195–208.

Katsanos, E., Sextos, A., and Manolis, G. (2010). "Selection of earthquake ground motion records: A state-of-the-art review from a structural engineering perspective." *Soil Dyn. Earthquake Eng.*, 30(4), 157–169.

Kawashima, K. (2010). "Seismic damage in the past earthquakes, seismic design of urban infrastructure." Lecture note, ⟨http://seismic.cv.titech.ac.jp/en/lecture/seismic_design/⟩, (Dec. 2, 2010).

Kent, D. C., and Park, R. (1971). "Flexural members with confined concrete." *J. Struct. Div.*, 97(7), 1969–1990.

Lee, T. H., and Mosalam, K. M. (2004). "Probabilistic fiber element modeling of reinforced concrete structures." *Comput. Struct.*, 82(27), 2285–2299.

Lee, T. H., and Mosalam, K. M. (2006). "Probabilistic seismic evaluation of reinforced concrete structural components and systems." PEER *Technical Report 2006/04*, Pacific Earthquake Engineering Center, Berkeley, CA.

Lessloss-Risk Mitigation for Earthquakes and Landslides Integrated Project. (2007). "Guidelines for displacement-based design of building and bridges." *LESSLOSS Report No. 2007/05*, IUSS Press, Pavia, Italy.

Liel, A., Haselton, C., Deierlein, G. G., and Baker, J. W. (2009). "Incorporating modeling uncertainties in the assessment of seismic collapse risk of buildings." *Struct. Saf.*, 31(2), 197–211.

Lupoi, A., Franchin, P., and Schotanus, M. I. J. (2003). "Seismic risk evaluation of RC bridge structures." *Earthquake Eng. Struct. Dyn.*, 32(8), 1275–1290.

Mander, J. B., Priestley, M. J. N., and Park, R. (1988). "Theoretical stress–strain model for confined concrete." *J. Struct. Eng.*, 114(8), 1804–1826.

McKenna, F., Fenves, G. L., and Scott, M. H. (2006). *OpenSees: Open system for earthquake engineering simulation*, Pacific Earthquake Engineering Center, Univ. of of California, Berkeley, ⟨http://opensees.berkeley.edu/⟩.

Menegotto, M., and Pinto, P. E. (1973). "Method for analysis of cyclically loaded reinforced concrete plane frames including changes in geometry and non-elastic behavior of elements under combined normal force and bending." *Proc., International Association for Bridge and Structural Engineering*, Lisbon, Portugal.

Nowak, A. S., and Szerszen, M. M. (1998). "Bridge load and resistance models." *Eng. Struct.*, 20(11), 985–990.

Pacific Earthquake Engineering Center (PEER). (2006). PEER strong motion database. ⟨http://peer.berkeley.edu/smcat⟩.

Pacific Earthquake Engineering Center (PEER). (2009). "Evaluation of ground motion Selection and modification methods: Predicting median interstory drift response of buildings." *Report PEER 2009/01*, PEER Ground Motion Selection and Modification Working Group, C. B. Haselton, ed., Univ. of California, Berkeley.

Padgett, J. E., and DesRoches, R. (2007). "Sensitivity of seismic response and fragility to parameter uncertainty." *J. Struct. Eng.*, 133(12), 1710–1718.

Padgett, J. E., and DesRoches, R. (2008). "Methodology for the development of analytical fragility curves for retrofitted bridges." *Earthquake Eng. Struct. Dyn.*, 37(8), 1157–1174.
Saltelli, A., Chan, K., and Scott, M., eds. (2000). *Sensitivity Analysis*, Wiley, New York.
Scott, M. H., and Fenves, G. L. (2006). "Plastic hinge integration methods for force-based beam-column elements." *J. Struct. Eng.*, 132(2), 244–252.
Shome, N., Cornell, C. A., Bazzurro, P., and Carballo, J. (1998). "Earthquake, records, and nonlinear responses." *Earthquake Spectra*, 14(3), 469–500.
Tabsh, S. W. (1996). "Reliability of composite steel bridge beams designed following AASHTO's LFD and LRFD specifications." *Struct. Saf.*, 17(4), 225–237.
Tubaldi, E., Barbato, M., and Dall'Asta, A. (2010). "Transverse seismic response of continuous steel–concrete composite bridges exhibiting dual load path." *Earthquakes Struct.*, 1(1), 21–41.
Vamvatsikos, D., and Cornell, C. A. (2002). "Incremental dynamic analysis." *Earthquake Eng. Struct. Dyn.*, 31(3), 491–514.
Vamvatsikos, D., and Fragiadakis, M. (2010). "Incremental dynamic analysis for estimating seismic performance sensitivity and uncertainty." *Earthquake Eng. Struct. Dyn.*, 39(2), 141–163.